

available at [www.sciencedirect.com](http://www.sciencedirect.com)journal homepage: [www.ejconline.com](http://www.ejconline.com)

# Magnetic functionalised carbon nanotubes as drug vehicles for cancer lymph node metastasis treatment

Feng Yang <sup>a,b,e</sup>, Chen Jin <sup>a,b,e</sup>, Dong Yang <sup>c</sup>, Yongjian Jiang <sup>a,b</sup>, Ji Li <sup>a,b</sup>, Yang Di <sup>a,b</sup>, Jianhua Hu <sup>c</sup>, Changchun Wang <sup>c</sup>, Quanxing Ni <sup>b,d</sup>, Deliang Fu <sup>a,b,\*</sup>

<sup>a</sup> Pancreatic Disease Institute, Department of Pancreatic Surgery, Huashan Hospital, Shanghai Medical College, Fudan University, Shanghai 200040, China

<sup>b</sup> Department of Surgery, Shanghai Medical College, Fudan University, Shanghai 200032, China

<sup>c</sup> Department of Macromolecular Science, Key Laboratory of Molecular Engineering of Polymers Ministry of Education, Laboratory of Advanced Materials, Fudan University, Shanghai 200433, China

<sup>d</sup> Pancreatic Disease Institute, Department of Pancreatic and Hepatobiliary Surgery, Cancer Hospital, Shanghai Medical College, Fudan University, Shanghai, 200032, China

## ARTICLE INFO

### Article history:

Received 27 October 2010

Received in revised form 14 March 2011

Accepted 15 March 2011

Available online 13 April 2011

### Keywords:

Carbon nanotubes

Cancer

Lymph node metastasis

Gemcitabine

Magnetic targeted

## ABSTRACT

Strategies using carbon-based nanomaterials as carriers for delivering chemotherapeutic drugs to cancers have been described well. Here a novel magnetic lymphatic-targeting drug-delivery system, based on functionalised carbon nanotubes (fCNTs), is presented with the aim of improving the outcome of cancer with lymph node involvement. The potential therapeutic effect of gemcitabine (GEM) loading magnetic multiwalled carbon nanotubes (mMWNTs) was compared with that of GEM loading magnetic-activated carbon particles (mACs) *in vitro* and *in vivo*. mMWNTs-GEM and mACs-GEM both had high anti-tumour activity *in vitro* similar to free drug. Subcutaneous administration of GEM loading magnetic nanoparticles resulted in successful regression and inhibition of lymph node metastasis under the magnetic field, with mMWNTs-GEM superior to mACs-GEM, and more effectively in the high-dose versus low-dose groups. The successful application of intra-lymphatic delivery of chemotherapeutics using mMWNTs highlights the clinical potential of fCNTs for future cancer metastasis treatment with high efficacy and minimum side-effects.

© 2011 Elsevier Ltd. All rights reserved.

## 1. Introduction

A variety of cancers are associated with high incidence of lymph node metastasis, which may occur at an early stage. Although many measures have been taken to improve the outcome, the effectiveness of current methods remains limited. Most studies have not demonstrated that aggressive surgery is associated with benefit in long-term survival. And so far, clinical evidence has not demonstrated the beneficial

effects of chemotherapy or radiotherapy for cancer lymph node metastasis. Furthermore, these interventions may yield many side-effects because of their toxicities. Therefore, it is urgent to investigate novel strategies to eradicate metastatic cancer cells from the regional lymph nodes.

Recently, chemotherapy targeting regional lymph nodes has emerged as a promising strategy for the treatment of malignancies, such as breast, gastric, rectal and intraperitoneal cancers,<sup>1</sup> which have high tendency to lymphatic metas-

\* Corresponding author at: Pancreatic Disease Institute, Department of Pancreatic Surgery, Huashan Hospital, Fudan University, Shanghai 200040, China.

E-mail address: [surgeonfu@yahoo.com.cn](mailto:surgeonfu@yahoo.com.cn) (D. Fu).

<sup>e</sup> These authors contributed equally to this work.

0959-8049/\$ - see front matter © 2011 Elsevier Ltd. All rights reserved.

doi:10.1016/j.ejca.2011.03.018

tasis. Despite that results seemed promising for prevention of recurrence and metastasis by using lymphotropic drug carriers such as activated carbons (ACs) or liposomes,<sup>2</sup> many interesting issues concerning more specific aspects of this technique remain to be further addressed, such as tumour cell targeting and high efficiency with low dosage.

Functionalised carbon nanotubes (fCNTs) have the potential for medical research and application. They have plenty of inner spaces where the incorporation of drugs is possible, and on the tube walls of carbon nanotubes (CNTs), drugs and various functional molecules can be physically adsorbed. Furthermore, the edges of the tube holes have oxidised functional groups where covalent attachment of chemicals is possible.<sup>3</sup> CNTs have been proved to be versatile carriers for various drugs, such as doxorubicin,<sup>4</sup> carboplatin<sup>5</sup> and paclitaxel.<sup>6</sup> Magnetic CNTs have also shown promising results as a MRI contrast agent with high nuclear magnetic resonance relaxivities, little cytotoxicity and high cell-labelling efficiency.<sup>7</sup> Most recently, CNTs and carbon nanohorns have been tested as anticancer drug carriers, gene vectors and thermal ablation agents for *in vivo* cancer treatment.<sup>3,6,8–11</sup>

In previous research we have demonstrated that poly(acrylic acid) functionalised multi-walled carbon nanotubes (PAA-g-MWNTs) decorated with magnetite nanoparticles ( $\text{Fe}_3\text{O}_4$ ) can be efficiently taken up by lymphatic vessels and delivered to regional lymph nodes *in vivo* with little toxicities.<sup>1</sup> In addition, this magnetic lymphatic targeting system<sup>12</sup> can deliver gemcitabine (GEM) into the lymph nodes *in vivo* with high efficiency under the guidance of magnetic field.<sup>13</sup> GEM is a nucleoside analogue and a S-phase specific cytotoxic agent shown activity in many solid tumours, such as pancreatic cancer, non-small cell lung cancer, head and neck squamous cell cancer, germ cell tumours, and tumours of the bladder, breast, ovary, cervix and biliary tract, as well as some haematologic malignancies.<sup>14</sup> Herein, we further investigated whether this novel lymphatic targeting drug delivery system using functionalised mMWNTs can be effective for cancer treatment.

## 2. Materials and methods

### 2.1. Functionalisation of multi-walled carbon nanotubes and gemcitabine loading

Multi-walled carbon nanotubes (MWNTs, purity >95%), produced by chemical vapour deposition (CVD) method, were purchased from Shenzhen Nanotech Port Co., Ltd. The preparation of magnetic poly(acrylic acid) (Fig. 1A) functionalised MWNTs (mMWNTs) (Fig. 1B) and its characterisation have been described previously.<sup>1,13</sup> Transmission electron microscope (TEM) analysis of mMWNTs revealed the  $\text{Fe}_3\text{O}_4$  nanoparticles (diameter of 8–12 nm) were clearly evident on the outer surface of the MWNTs with a bundle diameter of 40–60 nm. X-ray diffraction spectra of mMWNTs confirmed that the nanoparticles attached on the outer surface of PAA-g-MWNTs were  $\text{Fe}_3\text{O}_4$ .<sup>13</sup> The magnetic properties measured by a vibrating sample magnetometer showed that mMWNTs had superparamagnetic behaviour. After being dried under vacuum, mMWNTs were dissolved in sterilised water containing (polyvinylpyrrolidone) PVP-K30 as stabilizing agent

in a beaker by sonication for 30 min and stirring for 2 h at room temperature. GEM (purity >99%, Hansen Pharm, Jiangsu) was mixed into this solution by sonicating and stirring for 60 min, with a weight ratio of mMWNTs to GEM 5:2. The drug loading efficiency for the mMWNTs-GEM was about 62%.<sup>13</sup> Sterilisation procedures with  $\gamma$ -rays irradiation were used in order to obtain bacteria/spore-free suspensions.<sup>15</sup>

### 2.2. Preparation of magnetic activated carbon particles and gemcitabine loading

The preparation and characterisation of magnetic activated carbon particles (mACs) have also been mentioned previously.<sup>1</sup> mACs had a mean diameter of about 30 nm detected by TEM. The proportion of each corresponding ingredient in mACs was the same as that in mMWNTs. GEM was added into the mACs suspension by sonicating and stirring for 60 min at room temperature, with a weight ratio of mACs to GEM 5:2.

### 2.3. Cell culture

The human pancreatic cancer cell lines BxPC-3 and SW1990 (from the American Type Culture Collection) were used in this study. Cells were cultivated in 75 cm<sup>2</sup> culture flasks (Corning Costar) in RPMI 1640 culture medium (Gibco BRL-Life Technologies), supplemented with 10% heat-inactivated foetal bovine serum, 100 U/ml penicillin and 100 U/ml streptomycin, at 37 °C in 5% CO<sub>2</sub> and 95% air atmosphere and >95% humidity and were harvested when they were in logarithmic growth.

### 2.4. In vitro cytotoxicity

Cells were trypsinised and seeded into 96-well plates at 5000 cells/ml per well. After 24 h the medium was replaced with fresh medium containing different concentrations of only mACs, mACs-GEM (based on GEM concentration), only mMWNTs, mMWNTs-GEM (based on GEM concentration), or GEM alone, respectively. The *in vitro* cell cytotoxicity after various treatments was assessed at given time intervals (12, 24 and 48 h) by the 3-(4,5-dimethylthiazol-2-yl)-2,5-diphenyltetrazolium bromide (MTT) assay. The MTT assay was done in triplicates for each drug concentration used. After addition of 20  $\mu$ l/well of 5 mg/ml MTT solution (Sigma) for 4 h, the supernatant was removed carefully and 150  $\mu$ l DMSO was then added. After mixing for certain minutes on a horizontal shaker, the absorbance of the supernatant was measured at 490 and 570 nm. Cultures without cells were used as blanks. The percentage of cell viability was calculated as a ratio of OD of drugs-treated cells and control cells (treated with DMSO vehicle).

### 2.5. Transmission electron microscopy (TEM)

The ultrastructural alterations of cancer cells induced by the nanoparticles were observed with Hitachi H-600 transmission electron microscope (TOSHIBA, Japan). BxPC-3 and SW1990 cells were incubated in 75-cm<sup>2</sup> plastic culture flasks until 80% confluence. After a 48 h exposure of drugs, cells were washed with PBS, and fixed with 2.5% glutaraldehyde in 0.045 M sodium cacodylate buffer at 4 °C. After being washed

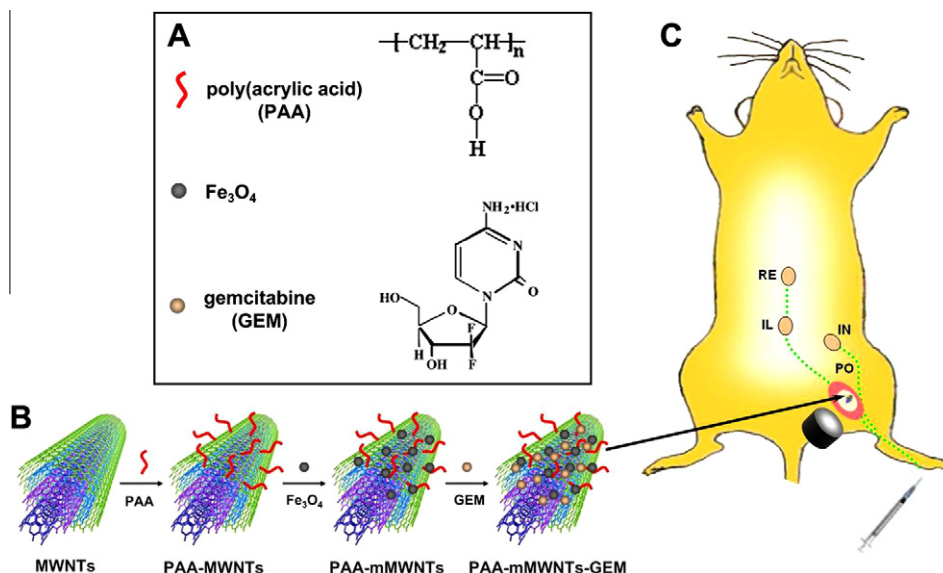


**Fig. 1 – Magnetic lymphatic drug delivery system. (A) Molecular structures of poly(acrylic acid) and gemcitabine (GEM). (B) Schematic synthetic route of magnetic multiwalled carbon nanotubes (mMWNTs) and illustration of chemical reactions used to attach gemcitabine onto mMWNTs. (C) Schematic drawing of magnetic lymphatic targeted chemotherapy in mice. mMWNTs-GEM were subcutaneously injected into a mouse that had cancer lymph node metastasis via the left rear footpad, and were taken up into lymphatic vessels and retained in the targeted lymph node under the magnetic field. For clarity, different parts are drawn at arbitrary scales. PO, popliteal lymph node; IN, inguinal lymph node; IL, para-iliac lymph node; RE, renal hilar lymph nodes.**

with cacodylate buffer, the cells were postfixed with 1% osmium tetroxide at 4 °C for 2 h. The cells were then dehydrated in a graded ethanol series and replaced in propylene oxide. After infiltration and embedding in epoxy resins at 60 °C for 48 h, ultrathin sections were performed using ultramicrotome. Then, the sections were stained with lead citrate and observed with the TEM at 120 kV.

## 2.6. Animal model and treatment protocol

Six to eight week old athymic nude male mice (BALB/c nu/nu) were purchased from Shanghai SLAC Laboratory Animal Co., Ltd, China and housed in a specific pathogen-free animal facility. All animal procedures were approved by the institutional animal care committee. All guidelines met the ethical standards required by law and also complied with the guidelines for the use of experimental animals in China. The preparation of lymph node metastasis model of pancreatic cancer has previously been described.<sup>1</sup> Briefly, a cell line with high metastatic capacity to the lymph nodes was established by sequential passages of BxPC-3 through the nude mouse. The metastatic nude-mouse model was obtained by inoculating subcutaneously into the left hind footpad with 0.05 ml of this highly metastatic cell line ( $5 \times 10^7$ /ml). The mice were used for treatment when the tumour diameter reached 8 to 10 mm with neither ulceration nor necrosis (~4 weeks after tumour inoculation).

To evaluate the inhibitory effects on lymph node metastasis, the mice were randomly divided into ten groups (six mice per group): GEM using mMWNTs as drug carrier with (mMWNTs-GEM-Mag) and without (mMWNTs-GEM) applying implanted *in vivo* magnets, and GEM using mACs as drug carrier with (mACs-GEM-Mag) and without (mACs-GEM) applying implanted *in vivo* magnets, saline, mACs, mMWNTs

and GEM treated groups were used as controls. Both of the formulations of GEM in the mMWNTs-GEM-Mag and mACs-GEM-Mag groups were injected at two doses normalised to be 6 and 12 (high dose group) mg/kg GEM equivalent, respectively (Table 1). The groups containing mACs had the same concentration as mMWNTs groups. At the day before treatment, a permanent magnet of 1800 Gs was sutured near the left popliteal lymph nodes in the groups of applying implanted *in vivo* magnets (Fig. 1C). For the treatment, 40–60  $\mu$ L of different formulations of GEM were subcutaneously injected into mice via the left rear footpad every 7 days for two times. At 15th day post-initial administration, mice were sacrificed and the popliteal lymph nodes were collected. The metastatic lymph nodes were weighed using electronic balance and measured by a vernier caliper, and calculated as the volume = (length)  $\times$  (width)<sup>2</sup>/2.

## 2.7. Histopathological examination of the metastatic lymph nodes

The lymph nodes removed from each animal were fixed in 10% formalin, and then processed for paraffin embedding. 5  $\mu$ m thick slices were cut and then stained by standard haematoxylin eosin (H&E) and immunohistochemical methods, respectively. The immunohistochemical staining of the lymph nodes was evaluated using a monoclonal mouse antibody against human cytokeratin (clone LP34, Dako, Denmark), employing routine immunoperoxidase techniques. Briefly, the deparaffinised tissue sections were boiled in 10 mmol/L, pH 6 citrate buffer for 20 minutes in a microwave oven. Endogenous peroxidase was blocked by incubation of the slides at room temperature with 0.3%  $H_2O_2$  in methanol. The slides were incubated with monoclonal anti human cyto-

**Table 1 – Different experimental groups and their treatment protocols.**

Groups	GEM dosage (mg/kg)	Magnet
Control	0	Without
mACs	0	Without
mMWNTs	0	Without
GEM	6	Without
mACs-GEM	6	Without
mMWNTs-GEM	6	Without
mACs-GEM-Mag	6	With
mMWNTs-GEM-Mag	6	With
mACs-GEM(HD)-Mag	12	With
mMWNTs-GEM(HD)-Mag	12	With

HD indicated high dose; Mag indicated Magnet.

keratin at room temperature. Sections were then washed with PBS buffer, and a secondary Envision antimouse antibody (DAKO) was applied for 30 minutes at 37 °C. Sections were then washed and reacted with 3,3'-diaminobenzidine tetrahydrochloride and H<sub>2</sub>O<sub>2</sub>. Slides were finally counterstained with haematoxylin, dehydrated and mounted.

After cytokeratin immunohistochemical staining (CK-IHC), quantification of positively stained cells was evaluated on three high-powered fields from each section by computer-assisted image analysis.<sup>16</sup> Digitised images were obtained by using an Olympus BH2 light microscope equipped with a MicroFire digital camera. Quantitative analysis was performed using Image Pro Plus programs. Specific areas of interest were selected, including the total tissue section. The region covered by diaminobenzidine was quantified (positive area) and the mean optical density of the positive region determined. The latter parameter determines average intensity of the selected colour in the region of interest. Protein expression (CK-IHC index) was determined by multiplying the positive area by the mean optical density.

Terminal deoxynucleotidyl transferase-mediated dUTP nick end-labelling (TUNEL) staining was performed using the *In Situ* Cell Death Detection Kit (Roche) according to the manufacturer's instructions. A total of 1000 cells were counted from randomly chosen high power microscopic fields for each sample, and the apoptotic index was calculated as the percentage ratio between the number of cells displaying apoptotic appearance and the total number of counted cells.

## 2.8. *In vivo* toxicity studies

Skin reactions at injection sites, body weight and behaviours of mice were recorded during the whole experiment. Blood samples were collected at time of sacrifice for analysis of blood serum chemistries. The blood samples were analysed using an automatic haematological analyser, ADVIA120 (Bayer, Germany). Serum samples were obtained from blood by centrifugation (3000 rpm for 15 min). Serum creatinine (Scr) and alanine aminotransferase (ALT) were determined by a fully automatic biochemical analyser (BTS 370, Spain).

## 2.9. Statistical analysis

Data were expressed as mean values  $\pm$  standard deviation (SD). Statistical analysis of this study was performed with AN-

OVA using SPSS 11.5 software. Values of  $P < 0.05$  were considered to be statistically significant.

## 3. Results

### 3.1. Effects of mMWNTs on cell viability

The *in vitro* cytotoxicities of only mACs, mACs-GEM, only mMWNTs and mMWNTs-GEM against SW1990 and BxPC-3 cancer cells were investigated together with a positive control of GEM alone. The inhibitory rate was determined after 48h of incubation with a series of doses of only mACs, mACs-GEM, only mMWNTs, mMWNTs-GEM and GEM alone. The results indicated that both mACs and mMWNTs had minimal effects on SW1990 and BxPC-3 cells even at high concentration of 25  $\mu$ g/ml, suggesting the relatively non-toxic nature of these compounds on the cancer cells (Fig. 2A and B). As indicated in Fig. 2C and D, treatment of the cancer cells with various concentrations (0.001, 0.01, 0.1, 1, and 10  $\mu$ g/ml GEM) of mACs-GEM and mMWNTs-GEM caused a dose-dependent decrease in cell viability relative to the control culture, which was similar to GEM alone. Although mMWNTs-GEM exhibited a little improved cytotoxicity compared with GEM at the equivalent of GEM 1 or 10  $\mu$ g/ml (Fig. 2A and B), there were no significances amongst mMWNTs-GEM, mACs-GEM and GEM at equal GEM concentrations. All these indicate that the activity of GEM was not adversely influenced during the preparation process, and cytotoxic effects of the main active components from mMWNTs-GEM and mACs-GEM were GEM. As the dose of nanoparticles in the medium reached 10  $\mu$ g/ml and cultured for 48 h, mMWNTs were internalised by BxPC-3 cells and located in the perinuclear region (Fig. 3A and B). mACs could also be taken by endocytosis inside the vesicles in the cytoplasm and morphology of the cells remained normal. The mACs inside the vesicles formed clusters (Fig. 3C and D).

### 3.2. Magnetic nanoparticles enhance *in vivo* therapeutic effect of gemcitabine

We evaluated the antitumour activity of magnetic nanoparticles, together with GEM *in vivo*, using the lymph node metastasis model. Under our experimental protocol, administration of mMWNTs and mACs caused no reductions on the metastatic lymph node volume. In addition, relative to control



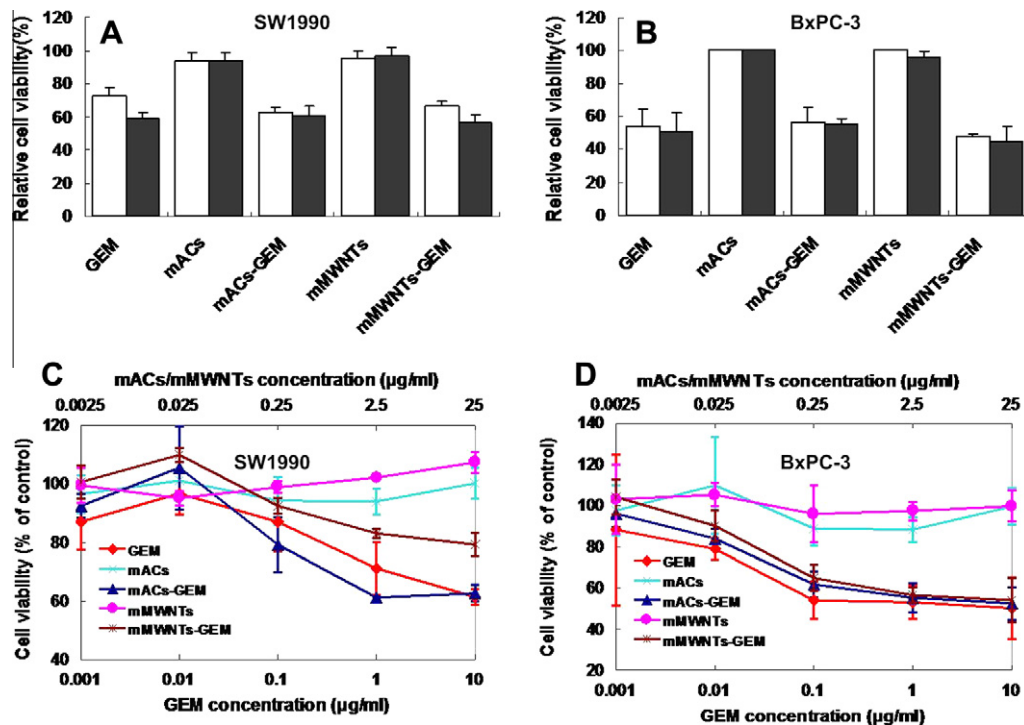


**Fig. 2** – *In vitro* growth inhibitory activities of gemcitabine, mACs, mACs-GEM, mMWNTs, and mMWNTs-GEM. Antiproliferation effects of gemcitabine, mACs, mACs-GEM, mMWNTs, and mMWNTs-GEM at two concentrations (□ gemcitabine 1 µg/ml, mACs/mMWNTs 2.5 µg/ml; ■ gemcitabine 10 µg/ml, mACs/mMWNTs 25 µg/ml) in SW1990 (A) and BxPC-3 (B) cells. The percentage of cell viability was calculated as a ratio of OD of drug-treated cells and control cells. Data were expressed as mean  $\pm$  standard deviation (SD). SW1990 (C) and BxPC-3 (D) cells viability curve measured by MTT assay after 48 h incubation with various concentrations of gemcitabine, mACs, mACs-GEM, mMWNTs, and mMWNTs-GEM. Points, mean; Bars, SD. The experiments for the two cells lines were done in identical conditions for comparison.

group, GEM treatment alone also caused no reduction ( $P > 0.05$ ) in lymph node volume. However, under identical experimental conditions, mMWNTs-GEM and mACs-GEM showed marked decrease in lymph node volume relative to the control group regardless of the magnet's existence, except the mACs-GEM group. The results were consistent with the effects on lymph node weight. Of interest, mMWNTs-GEM achieves better efficacy than mACs-GEM. A progressive decline in lymph node volume, as well as lymph node weight, was apparently evident in the groups with magnet or using high dose GEM as represented in Fig. 4.

### 3.3. Tumour histology and immunohistochemistry

H&E evaluation of the lymph nodes from all the groups showed neoplastic cells with marked nuclear atypia, which mostly arranged in a cord-like or nest-like distribution. Various degrees of tumour apoptosis and necrosis were present in the lymph nodes. The black nanoparticles were mainly located around the metastatic foci (Fig. 5C). To investigate the tumour suppression mechanism, we performed TUNEL assay to measure proportions of apoptotic cancer cells in the lymph nodes<sup>17</sup> from mice that received different treatments. The cancer cells in the control group showed the lowest degree of apoptosis. Similar to the control group, mMWNTs or mACs treated group showed only 8.2% and 6.4% of apoptotic cells. In contrast, in the groups receiving mMWNTs-GEM and mACs-

GEM, there were increased degrees of apoptosis, with the mMWNTs-GEM(HD)-Mag group having the highest apoptosis level (22%;  $P < 0.05$  versus the mMWNTs-GEM group). Similar but lower apoptosis level was seen in the mMWNTs-GEM-Mag group (20.2%;  $P < 0.01$  versus the GEM group). The groups receiving mMWNTs-GEM had higher apoptosis levels than those receiving mACs-GEM when applying implanted *in vivo* magnets at either dosage (Fig. 5A). Recent studies demonstrated that micrometastasis to regional lymph nodes in various cancers could be detected by CK-IHC.<sup>18–21</sup> We evaluated the distribution of cancer cells within the lymph nodes using CK antibody staining. As expected, the control group had the highest CK-IHC index ( $87420.8 \pm 6675.9$ ), with a significant difference seen between the control group and all the other groups ( $P < 0.01$ ). Compared with the mMWNTs group ( $57484.4 \pm 8491.4$ ), the groups containing mMWNTs-GEM showed significant lower CK-IHC index ( $P < 0.05$  versus the mMWNTs-GEM group;  $P < 0.01$  versus the mMWNTs-GEM-Mag and mMWNTs-GEM(HD)-Mag groups). The same results were obtained when comparing the groups containing mMWNTs-GEM and the GEM group ( $P < 0.01$ ). Similar results but higher CK-IHC index was seen in the groups receiving mACs and mACs-GEM. Amongst the groups containing mMWNTs-GEM, the mMWNTs-GEM(HD)-Mag group had the lowest CK-IHC index ( $41009.3 \pm 15324.6$ ;  $P < 0.01$  versus the mMWNTs-GEM group), whilst no significant difference was seen between the mMWNTs-GEM-Mag and mMWNTs-

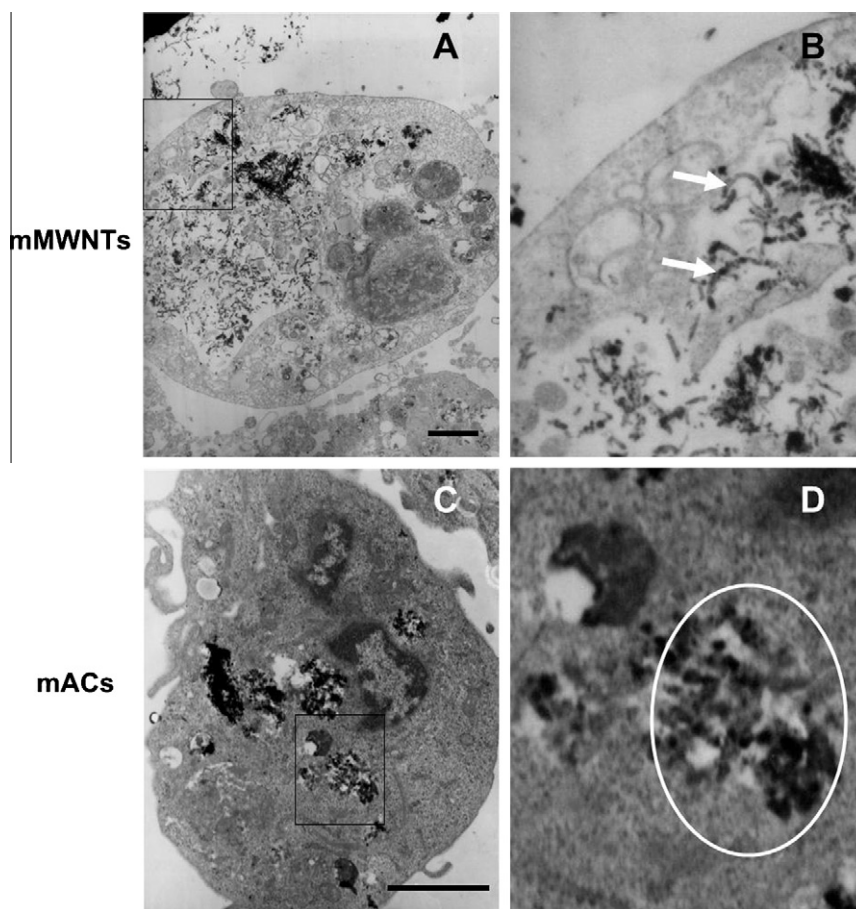


**Fig. 3 – TEM images of nanoparticles uptake.** Transmission electronic microscope micrographs of cancer cells which internalised nanoparticles. (A) mMWNTs treated BxPC-3 cells, (B) magnified image of the boxed region in (A). The white arrows point to mMWNTs inside the cytoplasm. (C) mACs treated SW1990 cells, (D) magnified image of the boxed region in (C). The white circle indicates aggregated mACs inside the vesicles. Scale bars are 2  $\mu$ m.

GEM(HD)-Mag groups ( $P > 0.05$ ) (Fig. 5B). No significance difference was noted with regard to the groups receiving mACs-GEM either in the magnetic field or not. The groups receiving mMWNTs-GEM had lower CK-IHC index than those receiving mACs-GEM under the magnetic field at either dosage, consistent with the TUNEL results.

### 3.4. Magnetic nanoparticles avoid side-effects

Our previous *in vivo* study found that foodpad injection of mACs and mMWNTs did not cause any obvious local or systemic toxicity in Sprague-Dawley rats, and no particle agglomerates were found in the major organs, whilst the nanoparticles accumulated in the draining lymph nodes and injection sites for a period of time.<sup>1</sup> Here, toxicity studies were carried out by treating tumour-bearing BALB/c mice with GEM, mACs-GEM and mMWNTs-GEM at the same GEM doses. During the course of administration, neither mortality nor noticeable behavioural changes of the mice were observed in the treated groups compared with the control group. No evidence of injection-site reactions such as superficial redness, drug allergy, infection, ulceration, erosion or necrosis of skin was observed, although particle accumulation in the injection sites was still found. No obvious body weight loss

was noted in all the groups, with body weight increase similar amongst the control and exposed groups. Blood chemistry tests showed that the haematological and serum biochemical parameters were within the normal ranges except for a slight decrease of white blood cells (WBC) in the GEM group. There was a significant difference in post treatment WBC counts between the groups with magnetic field exposure and the GEM group ( $P < 0.01$ ), suggesting that clinical applications of these magnetic nanoparticles could be safe (Table 2).

## 4. Discussion

Lymph node metastasis has been demonstrated as an important negative prognostic factor of cancers. The effectiveness of current strategies remains modest as the concentrations of the drugs in the lymph nodes are not enough to kill the cancer cells. Thus, developing novel formulation or delivery strategies of conventional chemotherapeutic agents for cancer metastasis receives much concern. Lymphatic chemotherapy may effectively increase and prolong the drug concentration in locoregional lymph nodes, which may lead to more effective tumour reduction in these areas and possibly lower locoregional recurrence and metastasis rates clinically, and has been considered as an ideal adjuvant therapy.

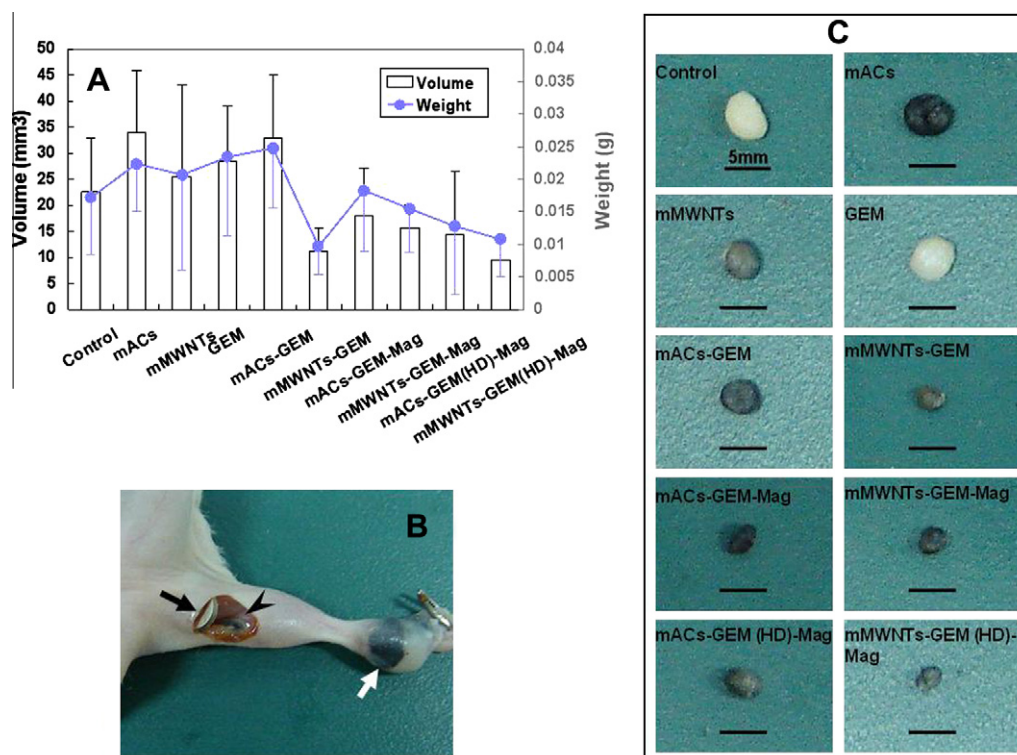


**Fig. 4 – In vivo lymph node targeting of the nanocomplexes and their therapeutic efficacies. (A) Effects of different treatment groups on metastatic lymph node growth inhibition in vivo.  $n = 6$  mice per treatment group. Points, mean of lymph node weight; bars, SD. (B) A representative photograph of the mouse to which mMWNTs-GEM were subcutaneously administered under the magnetic field. The primary tumour (white arrow), blackened metastatic popliteal lymph node (arrowhead), and magnet (black arrow) were shown. (C) Photographs of popliteal lymph nodes isolated on day 15 from mice treated with saline, mACs/mMWNTs, gemcitabine and various combinations with or without applying implanted in vivo magnets were shown. Scale bars are 5 mm.**

CNTs have been demonstrated to enable researchers to identify sentinel lymph nodes non-invasively in vivo.<sup>22–24</sup> Combined with their therapeutic characteristics, CNTs may play an important role in the theranostic nanomedicine<sup>25</sup> against cancer metastasis in future. In the present study, we used mACs and mMWNTs, which have been demonstrated capable of developing novel magnetic lymphatic-targeting drug-delivery systems, as drug vehicles to inhibit cancer lymph node metastasis. The results showed for the first time that mACs and mMWNTs effectively enhanced GEM cytotoxicity in vivo and inhibited lymph node metastasis, especially when using high dose agents and/or applying implanted in vivo magnets. The systems offer the possibility to enhance therapeutic effects and decrease side-effects associated with chemotherapeutic agents by utilising the synergistic effects of magnetic targeting and lymphatic chemotherapy.

In this study, mMWNTs and mACs showed little toxicities against BxPC-3 and SW1990 cells, which were in agreement with previous reports. Previous studies demonstrated that surface area and surface chemistry were the main variables that predicted the potential toxicities of carbon nanomaterials, and single-wall carbon nanotubes (SWNTs) induced stronger adverse effect than MWNTs.<sup>26–28</sup> The exact mechanisms that induce cellular toxicity are still unclear, but carbon-based nanomaterials can lead to cell death either after

contact with cell membranes or after their internalisation. The present study revealed that mMWNTs were able to cross cell membranes and affected drug transport. These phenomena could explain a few apoptotic cancer cells presented in the metastatic lymph nodes treated by mMWNTs or mACs alone.

CNTs have been investigated for possible applications in cancer treatment and can provide controlled targeting delivery of the chemotherapeutic agents with better efficacy and fewer side-effects.<sup>4–6,9–11</sup> In the present study, the therapeutic effectiveness of mMWNTs is better than that of mAC as drug carriers. The high efficacy of CNTs for the treatment of lymph node metastasis could be attributed to the following reasons. First, CNTs had high drug loading efficiency, and showed a higher efficiency in delivering GEM into the lymph nodes than mACs, especially under the magnetic field.<sup>13</sup> Second, mMWNTs displayed superparamagnetic behaviour with better targeting properties than mACs. Third, mMWNTs had the ability to cross cell membranes, which suggested that they can be used as intracellular transporters of biomolecules including proteins, DNA and drugs.<sup>29</sup> Kostarelos and colleagues<sup>30</sup> have demonstrated that functionalised CNTs seemed capable of cellular internalisation in all cell types and the nature of the functional group on the CNT surface did not determine whether func-



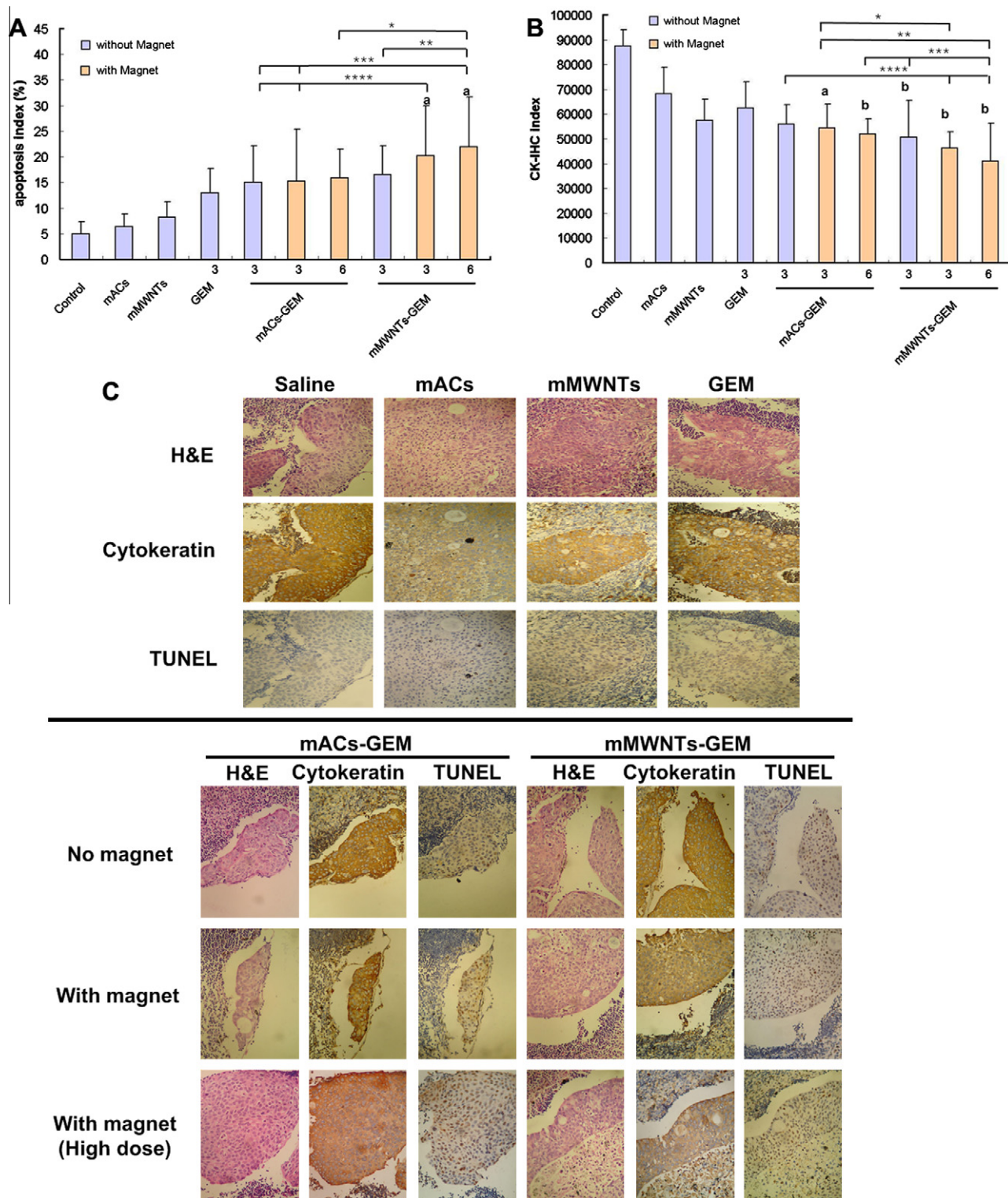


**Fig. 5** – H&E and immunohistochemical analysis of cytokeratin protein and apoptosis (terminal deoxynucleotidyl transferase-mediated dUTP nick end-labelling) in the metastatic lymph nodes harvested from tumour-bearing mice after subcutaneously administration of the drugs. (A) Apoptotic index was determined by the ratio of terminal deoxynucleotidyl transferase-mediated nick end-labelling-positive cells and total number of cells. Columns, mean; bars, SD. a  $P < 0.01$  compared with group GEM;  $^*P < 0.01$ ;  $^{**}P < 0.05$ ;  $^{***}P < 0.01$  compared with group mMWNTs-GEM(HD)-Mag;  $^{****}P < 0.05$  compared with group mMWNTs-GEM-Mag. (B) Quantification of cytokeratin-positive cells (CK-IHC index) evaluated by computer-assisted image analysis. Columns, mean; bars, SD. a  $P < 0.05$  compared with group GEM; b  $P < 0.01$  compared with group GEM;  $^*P < 0.05$ ;  $^{**}P < 0.01$ ;  $^{***}P < 0.01$  compared with group mMWNTs-GEM(HD)-Mag;  $^{****}P < 0.01$  compared with group mACs-GEM without magnet in vivo. (C) Representative light microscopic sections of the popliteal lymph nodes at the bottom (100×).



**Table 2 – Haematological and serum biochemical analysis in treated mice.**

Groups	WBC ( $\times 10^9$ /l)	RBC ( $\times 10^{12}$ /l)	Hb (g/l)	PLT ( $\times 10^9$ /l)	ALT (U/L)	Scr ( $\mu$ mol/l)
Control	4.77 $\pm$ 0.78	9.63 $\pm$ 0.83	11.2 $\pm$ 6.9	203.2 $\pm$ 117.9	60.0 $\pm$ 4.5	33.5 $\pm$ 2.1
mACs	4.46 $\pm$ 0.41	10.22 $\pm$ 0.36	15.1 $\pm$ 0.5	152.6 $\pm$ 29.1	63.5 $\pm$ 28.7	33.5 $\pm$ 3.2
mMWNTs	4.31 $\pm$ 1.33	9.29 $\pm$ 2.41	12.5 $\pm$ 6.2	194.1 $\pm$ 71.6	62.8 $\pm$ 30.3	32.8 $\pm$ 4.3
GEM	3.27 $\pm$ 1.24 <sup>a</sup>	9.86 $\pm$ 0.71	12.9 $\pm$ 4.6	152.6 $\pm$ 100.0	64.8 $\pm$ 15.5	33.7 $\pm$ 3.1
mACs-GEM	4.12 $\pm$ 1.66	9.80 $\pm$ 1.23	14.4 $\pm$ 1.6	180.0 $\pm$ 102.8	73.1 $\pm$ 18.1	29.8 $\pm$ 8.5
mMWNTs-GEM	5.11 $\pm$ 1.49	9.77 $\pm$ 0.98	12.5 $\pm$ 5.8	151.3 $\pm$ 86.9	65.8 $\pm$ 27.8	34.2 $\pm$ 8.0
mACs-GEM-Mag	7.15 $\pm$ 2.52 <sup>b</sup>	10.14 $\pm$ 0.49	14.6 $\pm$ 0.7	171.8 $\pm$ 59.3	67.6 $\pm$ 31.9	32.8 $\pm$ 8.5
mMWNTs-GEM-Mag	8.23 $\pm$ 2.60 <sup>b</sup>	10.31 $\pm$ 0.30	15.3 $\pm$ 0.4	159.0 $\pm$ 82.3	63.7 $\pm$ 25.3	28.0 $\pm$ 6.7
mACs-GEM(HD)-Mag	9.10 $\pm$ 4.18 <sup>b</sup>	10.15 $\pm$ 0.45	14.7 $\pm$ 1.0	163.4 $\pm$ 28.8	68.6 $\pm$ 17.8	26.9 $\pm$ 6.0
mMWNTs-GEM(HD)-Mag	8.50 $\pm$ 2.47 <sup>b</sup>	10.37 $\pm$ 0.32	14.7 $\pm$ 0.8	175.3 $\pm$ 85.7	56.6 $\pm$ 13.8	29.2 $\pm$ 8.2

All groups n = 6. Value of average  $\pm$  standard deviation.

ALT: Alanine aminotransferase; GEM: Gemcitabine; Hb: Haemoglobin; HD: high dose; Mag: Magnet; mACs: Magnetic activated carbon particles; mMWNTs: Magnetic multiwalled carbon nanotubes; PLT: Platelet; RBC: Red blood cell; Scr: Serum creatinine; WBC: White blood cell.

<sup>a</sup> Indicated results below the lower limits of normal range.

<sup>b</sup> Indicated there were statistically significant differences compared with GEM group ( $P < 0.01$ ).

tionalised CNTs were internalised or not. Cellular internalisation of CNTs takes an important role in targeting therapy for cancer; thus, understanding the exact internalisation mechanisms is crucial for pharmaceutical application of CNTs.<sup>29</sup> Although mACs have also been phagocytosed by the cancer cells in the experiment, the nanoparticle uptake is limited. Most recently, researchers have been developing CNTs coupled with cancer cell-specific targeting moieties to enhance CNTs uptake by cancer cells whilst limiting uptake by normal cells.<sup>9,12,31</sup>

The low toxicities of CNTs *in vivo* suggested that mMWNTs have the potential application as novel magnetic lymphatic-targeting drug-delivery system for treatment or prevention of tumour metastasis.<sup>6,32,33</sup> This pattern of magnetic lymphatic-targeting chemotherapy makes it possible to give drugs a durable effect, to prevent harmful side-reactions, and will have profound effects on time-controlled transport of drugs to lymph nodes. Most studies have reported that adverse effects of CNTs *in vivo* by intravenous administration, through which CNTs might be excreted from mice via the biliary and renal pathways, were resulted from their accumulation in major organs, such as liver and lung.<sup>1,32</sup> We injected the CNTs and carbon nanoparticles subcutaneously, and found no obvious nanoparticle agglomerates deposited in the lung, liver and spleen,<sup>1</sup> which is consistent with another recent study.<sup>34</sup> The fact that CNTs accumulated in the draining lymph nodes has raised concerns about their immunotoxicities. To investigate the immunological properties of CNTs, Meng and colleagues<sup>34</sup> injected oxidised water dispersible MWNTs in healthy BALB/c mice. Their results showed that MWNTs induced complement activation and production of proinflammatory cytokines early after injection, and that levels of complement and cytokines returned to normal over time. No injury was observed in the major organs or lymph nodes, except for accumulation of MWNTs in the lymph nodes. This study suggested that subcutaneous administration of CNTs might induce short-term immunological reaction and be relatively safer than the route of systemic injection. However, combining with their toxicological data on CNTs respiratory exposure, there is an urgent need for comprehensive assess-

ment of systemic effects, such as cardiovascular, neurological and immunological toxicities, before their clinical use.<sup>35,36</sup>

Superparamagnetic iron oxide nanoparticles have attracted a great deal of attention owing to their unique physicochemical properties and huge potential in cancer diagnosis and treatment, including MRI, controlled drug/gene delivery, and hyperthermia in cancer therapy.<sup>37</sup> Magnetic CNTs have also generated great excitement as they have been successfully used as vehicles to deliver biomolecules into mammalian cells,<sup>38</sup> MRI contrast agents; for cell labelling,<sup>7</sup> tracking haematopoietic stem and progenitor cell,<sup>39</sup> detecting circulating tumour cells<sup>40</sup>; and for hyperthermia applications.<sup>41</sup> mMWNTs, which simultaneously have lymphotropic and magnetic properties, belong to novel vehicles of magnetic targeted drugs delivery system. The principle of magnetic drug targeting has already been described by many researchers, whilst its application in humans is still in the starting stage.<sup>42</sup> We used mMWNT as chemotherapeutic agent vehicles to targeted cancer metastatic lymph nodes under the guide of implanted magnet. The results are encouraging, and provide scientists with theoretical and experimental bases for the treatment of cancer lymphatic metastasis using novel materials, formulations or approaches in the future. This method will allow for a more effective means of holding the chemotherapeutic drugs at the regional metastatic lymph nodes, and may provide us an opportunity to treat cancers locoregionally without systemic toxicity.

## Conflict of interest statement

None declared.

## Acknowledgements

This work was supported by the National Science Foundation of China (30901760, 81071884 and 50873029) the Program of Shanghai Subject Chief Scientist (08XD14010) and the Shanghai Educational Development Foundation (2008CG05).

## REFERENCES

- Yang F, Hu J, Yang D, et al. Pilot study of targeting magnetic carbon nanotubes to lymph nodes. *Nanomedicine (Lond)* 2009;4(3):317–30.
- Yang F, Jin C, Jiang Y, et al. Liposome based delivery systems in pancreatic cancer treatment: From bench to bedside. *Cancer Treat Rev* 2011 [Epub ahead of print].
- Ajima K, Murakami T, Mizoguchi Y, et al. Enhancement of in vivo anticancer effects of cisplatin by incorporation inside single-wall carbon nanohorns. *ACS Nano* 2008;2(10):2057–64.
- Ali-Boucetta H, Al-Jamal KT, McCarthy D, et al. Multiwalled carbon nanotube-doxorubicin supramolecular complexes for cancer therapeutics. *Chem Commun (Camb)* 2008(4):459–61.
- Hampel S, Kunze D, Haase D, et al. Carbon nanotubes filled with a chemotherapeutic agent: a nanocarrier mediates inhibition of tumor cell growth. *Nanomedicine (Lond)* 2008;3(2):175–82.
- Liu Z, Chen K, Davis C, et al. Drug delivery with carbon nanotubes for in vivo cancer treatment. *Cancer Res* 2008;68(16):6652–60.
- Bai X, Son SJ, Zhang S, et al. Synthesis of superparamagnetic nanotubes as MRI contrast agents and for cell labeling. *Nanomedicine (Lond)* 2008;3(2):163–74.
- Murakami T, Sawada H, Tamura G, et al. Water-dispersed single-wall carbon nanohorns as drug carriers for local cancer chemotherapy. *Nanomedicine (Lond)* 2008;3(4):453–63.
- Bhirde AA, Patel V, Gavard J, et al. Targeted killing of cancer cells in vivo and in vitro with EGF-directed carbon nanotube-based drug delivery. *ACS Nano* 2009;3(2):307–16.
- Podesta JE, Al-Jamal KT, Herrero MA, et al. Antitumor activity and prolonged survival by carbon-nanotube-mediated therapeutic siRNA silencing in a human lung xenograft model. *Small* 2009;5(10):1176–85.
- Burke A, Ding XF, Singh R, et al. Long-term survival following a single treatment of kidney tumors with multiwalled carbon nanotubes and near-infrared radiation. *Proc Natl Acad Sci USA* 2009;106(31):12897–902.
- Yang F, Fu D, Long J, Ni QX. Magnetic lymphatic targeting drug delivery system using carbon nanotubes. *Med Hypotheses* 2008;70(4):765–7.
- Yang D, Yang F, Hu JH, et al. Hydrophilic multi-walled carbon nanotubes decorated with magnetite nanoparticles as lymphatic targeted drug delivery vehicles. *Chem Commun* 2009:4447–9.
- Pauwels B, Korst AEC, Lardon F, Vermorken JB. Combined modality therapy of gemcitabine and radiation. *Oncologist* 2005;10(1):34–51.
- Bellucci S, Chiaretti M, Onorato P, et al. Micro-Raman study of the role of sterilization on carbon nanotubes for biomedical applications. *Nanomedicine (Lond)* 2010;5(2):209–15.
- Chabaud-Riou M, Firestein GS. Expression and activation of mitogen-activated protein kinase kinases-3 and -6 in rheumatoid arthritis. *Am J Pathol* 2004;164(1):177–84.
- Inbal B, Cohen O, Polak-Charcon S, et al. DAP kinase links the control of apoptosis to metastasis. *Nature* 1997;390(6656):180–4.
- El-Tamer M, Chun J, Gill M, et al. Incidence and clinical significance of lymph node metastasis detected by cytokeratin immunohistochemical staining in ductal carcinoma in situ. *Ann Surg Oncol* 2005;12(3):254–9.
- Cserni G, Bianchi S, Vezzosi V, et al. The value of cytokeratin immunohistochemistry in the evaluation of axillary sentinel lymph nodes in patients with lobular breast carcinoma. *J Clin Pathol* 2006;59(5):518–22.
- Ikeda S, Funakoshi N, Usui S, et al. Prognostic significance of gastric cancer metastasis in second-tier lymph nodes detected on reverse transcriptase-polymerase chain reaction and immunohistochemistry. *Pathol Int* 2008;58(1):45–50.
- Roder JD, Thorban S, Pantel K, Siewert JR. Micrometastases in bone marrow: prognostic indicators for pancreatic cancer. *World J Surg* 1999;23(9):888–91.
- Pramanik M, Song KH, Swierczewska M, et al. In vivo carbon nanotube-enhanced non-invasive photoacoustic mapping of the sentinel lymph node. *Phys Med Biol* 2009;54(11):3291–301.
- Kim JW, Galanzha EI, Shashkov EV, Moon HM, Zharov VP. Golden carbon nanotubes as multimodal photoacoustic and photothermal high-contrast molecular agents. *Nat Nanotechnol* 2009;4(10):688–94.
- Li JJ, Yang F, Guo GQ, et al. Preparation of biocompatible multi-walled carbon nanotubes as potential tracers for sentinel lymph nodes. *Polym Int* 2010;59(2):169–74.
- Sumer B, Gao J. Theranostic nanomedicine for cancer. *Nanomedicine (Lond)* 2008;3(2):137–40.
- Tian FR, Cui DX, Schwarz H, Estrada GG, Kobayashi H. Cytotoxicity of single-wall carbon nanotubes on human fibroblasts. *Toxicol In Vitro* 2006;20(7):1202–12.
- Magrez A, Kasas S, Salicio V, et al. Cellular toxicity of carbon-based nanomaterials. *Nano Lett* 2006;6(6):1121–5.
- Jia G, Wang HF, Yan L, et al. Cytotoxicity of carbon nanomaterials: Single-wall nanotube, multi-wall nanotube, and fullerene. *Environ Sci Technol* 2005;39(5):1378–83.
- Raffa V, Ciofani G, Vittorio O, Riggio C, Cuschieri A. Physicochemical properties affecting cellular uptake of carbon nanotubes. *Nanomedicine (Lond)* 2010;5(1):89–97.
- Kostarelos K, Lacerda L, Pastorin G, et al. Cellular uptake of functionalized carbon nanotubes is independent of functional group and cell type. *Nat Nanotechnol* 2007;2(2):108–13.
- Kam NWS, O'Connell M, Wisdom JA, Dai HJ. Carbon nanotubes as multifunctional biological transporters and near-infrared agents for selective cancer cell destruction. *Proc Natl Acad Sci USA* 2005;102(33):11600–5.
- Liu Z, Davis C, Cai W, et al. Circulation and long-term fate of functionalized, biocompatible single-walled carbon nanotubes in mice probed by Raman spectroscopy. *Proc Natl Acad Sci USA* 2008;105(5):1410–5.
- Ji SR, Liu C, Zhang B, et al. Carbon nanotubes in cancer diagnosis and therapy. *Biochim Biophys Acta* 2010;1806(1):29–35.
- Meng J, Yang M, Jia F, et al. Immune responses of BALB/c mice to subcutaneously injected multi-walled carbon nanotubes. *Nanotoxicology* 2010 [Epub ahead of print].
- Boczkowski J, Lanone S. Potential uses of carbon nanotubes in the medical field: how worried should patients be? *Nanomedicine (Lond)* 2007;2(4):407–10.
- Simeonova PP. Update on carbon nanotube toxicity. *Nanomedicine (Lond)* 2009;4(4):373–5.
- Lin MM, Kim HH, Kim H, Dobson J, Kim do K. Surface activation and targeting strategies of superparamagnetic iron oxide nanoparticles in cancer-oriented diagnosis and therapy. *Nanomedicine (Lond)* 2010;5(1):109–33.
- Cai D, Mataraza JM, Qin ZH, et al. Highly efficient molecular delivery into mammalian cells using carbon nanotube spearing. *Nat Methods* 2005;2(6):449–54.
- Gul H, Lu W, Xu P, et al. Magnetic carbon nanotube labelling for haematopoietic stem/progenitor cell tracking. *Nanotechnology* 2010;21(15):155101.
- Galanzha EI, Shashkov EV, Kelly T, et al. In vivo magnetic enrichment and multiplex photoacoustic detection of circulating tumour cells. *Nat Nanotechnol* 2009;4(12):855–60.
- Klingeler R, Hampel S, Buchner B. Carbon nanotube based biomedical agents for heating, temperature sensing and drug delivery. *Int J Hyperthermia* 2008;24(6):496–505.
- Krukemeyer MG, Wagner M, Jakobs M, Krenn V. Tumor regression by means of magnetic drug targeting. *Nanomedicine (Lond)* 2009;4(8):875–82.